Articles

T-State Active Site of Aspartate Transcarbamylase: Crystal Structure of the Carbamyl Phosphate and L-Alanosine Ligated Enzyme[†,‡]

Jingwei Huang and William N. Lipscomb*

Department of Chemistry and Chemical Biology, Harvard University, Cambridge, Massachusetts 02138

Received August 2, 2005; Revised Manuscript Received November 11, 2005

ABSTRACT: An X-ray diffraction study to 2.0 Å resolution shows that this enzyme, ATCase, is in the T-state (the c_3 to c_3 distance is 45.2 Å) when ATCase is bound to carbamyl phosphate (CP) and to L-alanosine (an analogue of aspartate). This result strongly supports the kinetic results that alanosine did not inhibit the carbamylation of aspartate in the normal reaction of native ATCase plus CP and aspartate [Baillon, J., Tauc, P., and Hervé, G. (1985) *Biochemistry 24*, 7182−7187]. The structure further reveals that the phosphate of CP is 4 Å away from its known position in the R-state and is in the T-state position of P_i in a recent study of ATCase complexed with products, phosphate (P_i) and *N*-carbamyl-L-aspartate [Huang, J., and Lipscomb, W. N. (2004) *Biochemistry 43*, 6422−6426]. Moreover, the alanosine position in this T-state is somewhat displaced from that expected for its analogue, aspartate, from the R-state position. The relations of these structural aspects to the kinetics are presented.

Aspartate transcarbamylase (ATCase)[1] from *Escherichia coli* (EC 2.1.3.2) catalyzed the reaction of L-aspartate with carbamyl phosphate to form carbamylaspartate and phosphate and initiates the pathway for pyrimidine biosynthesis. The holoenzyme of ATCase is composed of two catalytic trimers ($2c_3$, 102 kDa each) and three regulatory dimers ($3r_2$, 34 kDa each). The levels of intracellular pools of aspartate are estimated to be between 2 and 5 mM (*1*). The pH dependence of this catalyzed reaction varies with the concentration of L-aspartate (*2*−*7*): in the presence of low concentrations (≤5 mM) of L-aspartate, ATCase is essentially all in the T form (low affinity and low activity) and its optimum pH is 6.8, whereas in the presence of high concentrations of L-aspartate, ATCase is in the R form (high affinity and high activity) and its optimum pH is 8.2. A similar T-state reaction, which was catalyzed by ATCase, was also observed from the reverse reaction (*8*) under conditions in which the aspartate is rapidly removed by other enzymes, as well as from the reactions of carbamyl phosphate with L-aspartate analogues including cysteinesulfinate (*9*) or L-alanosine (*10*). When L-alanosine, an anticancer drug originally isolated from *Streptomyces alanosinicus* (*11*), was used as a substrate instead of L-aspartate, it has been reported that only a minor variation of pH dependence was observed (*10*): when the concentration for L-alanosine rose from 2 to 100 mM, the optimum pH remained between 6.8 and 7.0, and the saturation curve for L-alanosine did not exhibit homotropic cooperative interactions between the catalytic sites. The results have indicated that L-alanosine, for which K_m was estimated as higher than 1 M, reacted with carbamyl phosphate at an extremely low rate [$V = 0.28$ nmol min^{-1} (g of protein)$^{-1}$; carbamylalanosine was identified by chromatography (*10*) with a migration R_f value of 0.43] and was unable to promote the allosteric transition of ATCase (*10*). In the present study, the structure of ATCase complexed with carbamyl phosphate and L-alanosine is presented in order to compare the T-state ATCase complexes previously described with other ligands. Special attention is given to analogues of the physiological substrates, carbamyl phosphate and aspartate.

MATERIALS AND METHODS

Crystal Growth. The holoenzyme of *E. coli* aspartate transcarbamoylase was isolated by the method of Nowlan and Kantrowitz (*12*) from *E. coli* strain EK1104 containing the plasmid pEK54 (*13*). Carbamyl phosphate was purchased from the Sigma Chemical Co. The L-alanosine was a generous gift from Drs. D. Cooney, R. R. Davis, and V. Narayanan, Drug Synthesis and Chemistry Branch, Developmental Therapeutics Programs, Division of Cancer Treatment, NCI, Bethesda, MD. The crystals used in this study were grown at room temperature in the presence of 1 mM carbamyl phosphate and 1 mM L-alanosine by the hanging

[†] This work was supported by NIH Grant GM06920.

[‡] The coordinates have been deposited with the Protein Data Bank as 2AIR.

* To whom correspondence should be addressed. Phone: 617-495-4098. Fax: 617-495-3330. E-mail: lipscomb@chemistry.harvard.edu.

[1] Abbreviations: ATCase, aspartate transcarbamylase; PALA, *N*-phosphonacetyl-L-aspartate; CLA, *N*-carbamyl-L-aspartate; ALS, L-alanosine; AP, acetyl phosphate; CP, carbamyl phosphate; PDB, Protein Data Bank; 1D09, the R-state structure of aspartate transcarbamylase with PALA bound, deposited in the Protein Data Bank, determined to 2.1 Å resolution; 6AT1, the T-state structure of aspartate transcarbamylase deposited in the Protein Data Bank, determined to 2.6 Å resolution; CHESS, the Cornell High Energy Synchrotron Source.

10.1021/bi051543u CCC: $33.50
Published on Web 12/14/2005

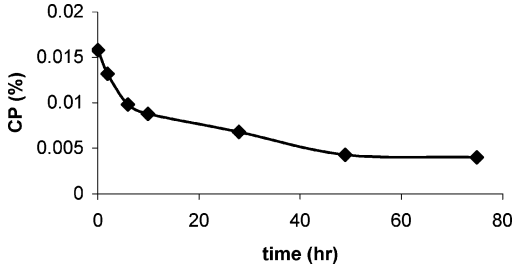

FIGURE 1: Decomposition of carbamyl phosphate at the buffer of 14% PEG 4000/0.1 M Hepes-Na (pH 7.5) measured by ^{32}P NMR, with 86% H_3PO_4 as the reference. The *Y*-axis is the concentration of CP relative to the reference.

drop method, where 2 μL of enzyme (16 mg/mL) in buffer (40 mM KH_2PO_4/0.2 mM EDTA/2 mM 2-mercaptoethanol, pH 7.0) was mixed with 2 μL of 12% (v/v) poly(ethylene glycol) 4000 (PEG-4K)/0.1 M Hepes-Na (pH 7.5)/4% (v/v) 2-propanol/3 mM NaN_3 and equilibrated against 1 mL of 14% PEG-4K/0.1 M Hepes-Na (pH 7.5)/4% (v/v) 2-propanol/3 mM NaN_3. Two days later, the crystals were frozen and stored under liquid nitrogen before the data collection. The decomposition of carbamyl phosphate has been measured in the crystallization buffer by ^{31}P NMR at room temperature. The result shows that the initial half-life of carbamyl phosphate is about 11 h, which is consistent with the previous experiment (*14*), and there is still about 25% of original carbamyl phosphate left after 3 days of the decomposition (Figure 1). This residual carbamyl phosphate is in equilibrium with phosphate and cyanate (*15*−*16*) under our crystallization buffer, and the result is close to the report of Halmann et al. (*17*). Successful cocrystallizations of carbamyl phosphate with ATCase (*14*) and OTCase (*18*) have been reported.

Data Collection and Analysis. The diffraction data were collected at 100 K on beamline F-1 of the Cornell High Energy Synchrotron Source (CHESS). Crystals of the ATCase complexed with carbamyl phosphate plus L-alanosine are in the space group R_3 and have unit cell dimensions of $a = b = 129.2$ Å, $c = 198.1$ Å, and $\gamma = 120°$. Diffraction data were collected to 2.0 Å, yielding an R_{merge} of 0.066 for 130959 measured reflections of 74502 unique reflections. The reduced data set was 89.5% complete in the resolution range 2.0−30 Å (Table 1).

A search model, which contains one catalytic chain and one regulatory chain (one-half of the asymmetric unit), was taken from PDB code 1D09 (*19*). Molecular replacement was carried out by AMoRe (*20*). A model of carbamyl phosphate (CP) was taken from PDB code 1C9Y (*21*), and the atomic coordinate of L-alanosine (ALS) was taken from the crystal structure of L-alanosine (*22*). Then, CP and ALS (Figure 2) were built into the simulated annealing omit map. The refinement was performed by using the CNS_SOLVE package (*23*). The model was visualized and modified against $2F_o - F_c$ and $F_o - F_c$ maps using the program O (*24*). The stereochemical properties of the intermediate and the final structures were examined by PROCHECK (*25*). Final refinement yielded $R = 0.239$, $R_{free} = 0.273$ for all diffraction data and $R = 0.207$, $R_{free} = 0.249$ for only 4σ cutoff data, and the Luzzati coordinate error of the final model is 0.25 Å. A total of 606 water molecules were found in one asymmetric unit. The protein−protein interface interactions were calculated by Protein−Protein Interaction Server (*26*) and checked by O. Figures 3 and 4 were prepared using PyMOL (*27*).

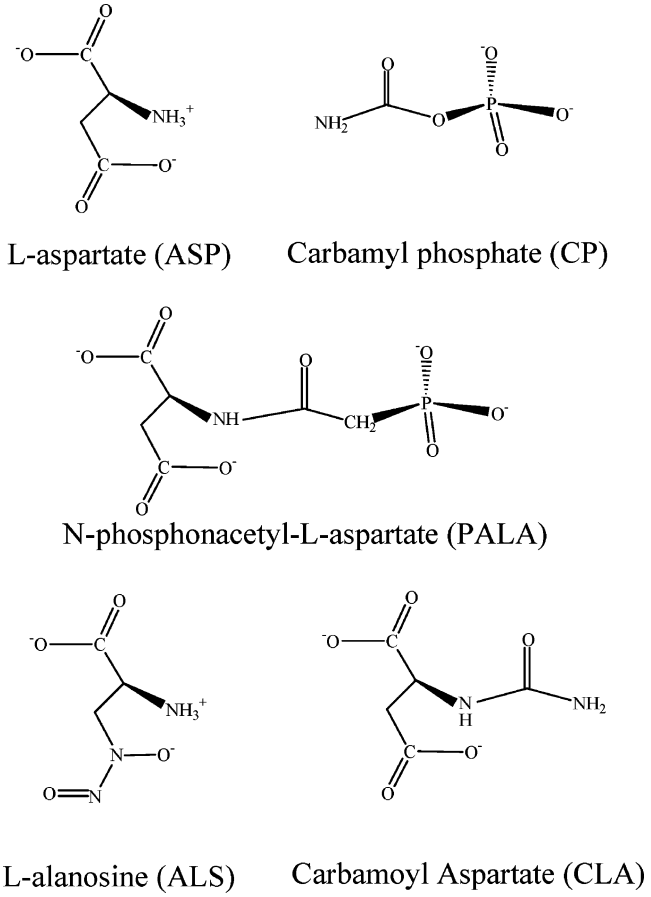

FIGURE 2: Chemical structures of the substrates and their analogues.

Table 1: Data Collection and Refinement Summary for Carbamyl Phosphate and L-Alanosine Ligated ATCase

crystal	
space group	R_3
cell dimensions	
a (Å)	129.2
b (Å)	129.2
c (Å)	198.1
γ (deg)	120
data collection	
resolution range (Å)	30−2.0
completeness (%)	89.5
average I/σ	10.7
R_{merge} (%)	6.6
refinement	
R/R_{free} (%)	23.9/27.3
reflections in the free *R* set	3363
Luzzati coordinate error (Å)	0.33
cross-validated error (Å)	0.44
rms deviations	
bond lengths (Å)	0.0069
bond angles (deg)	1.49

The planar angle *X*, which defines the hinge angle between domains, was calculated by the method of Williams et al. (*19*, *28*). Superposition of the structures and the relative rotation between domains were calculated by LSQMAN (*29*).

RESULTS

CP and L-Alanosine Are Unable To Promote ATCase to the R-State. The conformation of ATCase complexed with

Table 2: Relative Conformational Change of the ATCase Complex to Unligated ATCase[a]

	ATCase-CP-alanosine	ATCase-PALA (R-state)
$c_3\cdots c_3$ distance change (Å)	−0.1	10.8
c_3 to c_3 relative rotation (deg)	2	12
relative rotation of each r_2 (deg)	1.9	15
X-planar angle between domains		
Asp/CP (deg)	+1.2	−6.9
Zn/AL (deg)	+0.5	−1.7
CP/Zn (deg)	−0.6	−0.2
AL/AL (deg)	−3.4	+2.5

[a] The $c_3\cdots c_3$ distance of the unligated T-state ATCase (6AT1) is 45.3 Å. ATCase-CP-alanosine is a new structure of ATCase bound to CP and alanosine (2AIR). ATCase-PALA is the structure of ATCase bound to PALA (1D09). *X*-planar angles between domains define the hinge angle between domains (*19*, *28*); the minus means more closed and the plus means more open.

carbamyl phosphate plus L-alanosine is in the T-state; the catalytic trimer $c_3\cdots c_3$ distance is 45.2 Å, in excellent agreement with that in the unligated T-state of ATCase (45.3 Å; PDB code 6AT1) (*30*). The $c_3\cdots c_3$ distance is 56.1 Å in the R-state ATCase with its substrate analogue complexes (*19*). The global conformational differences between the new structure and the unligated T-state of ATCase (PDB code 6AT1) are indicated by the small relative rotation of the chains and the relative movements of domains, as follows. The c_3 to c_3 relative rotation around the 3-fold axis of trimers is about 2.0°, and the relative rotation of each regulatory chain around the pseudo-2-fold axis of regulatory dimers is about 1.9°; the *X*-planar angles between the Asp and CP domains are more open by 1.2°; the *X*-planar angles are only about 0.5° more open between the ZN and AL domains, and they are more closed by 0.6° between CP and ZN domains and more closed by 3.4° between the two AL domains. Compared to the big global conformational change by the transition from the T-state to the R-state (Table 2), these small differences support the assignment as the T form.

The T-state conformation is also indicated by the existence of the interactions Ser131−Asp236, Lys164−Glu239, and Tyr165−Glu239, which are conserved between two adjacent catalytic chains of two catalytic trimers in most T forms of ATCase. These bonds become broken when the enzyme conformation changes from the T-state to the R-state (*31*).

Active Sites of Carbamyl Phosphate and L*-Alanosine*. In each asymmetric unit of the new structure, there are two catalytic chains (indicated by chains A and G) and two regulatory chains (B and H). Each catalytic chain is ligated to one molecule of carbamyl phosphate (CP) and one molecule of L-alanosine (ALS). The two carbamyl phosphate molecules in one asymmetric unit are similar, as are the two L-alanosine molecules. The rms distance of Cα between chain A and chain G is 0.315 Å, and the rms distance of Cα between chain B and chain H is 0.762 Å.

In this T-state structure, the side chains of Arg54, Arg105, and His134 interact with the phosphate oxygens of carbamyl phosphate, and the side chains of Arg105 and His134 contact the carbamyl group of carbamyl phosphate. The side chain of Gln137 has a interaction with carbamyl phosphate in chain A as shown in Figure 3a, and the side chains of Thr55 and Arg229 are involved in the phosphate region of the carbamyl phosphate binding site in chain G as shown in Figure 3b.

Residues Thr53 and Arg53 interact with the *N*-nitroso-*N*-hydroxyamino group of L-alanosine, and residues Ala51 and Arg105 are in contact with the carboxyl group of L-alanosine. Residues Ser52 and *Ser80 from the adjacent catalytic chain (designated by the asterisk) are involved in the L-alanosine binding site in chain A (Figure 3a), and residues Glu50 and Thr55 are in close contact with L-alanosine in chain G (Figure 3b).

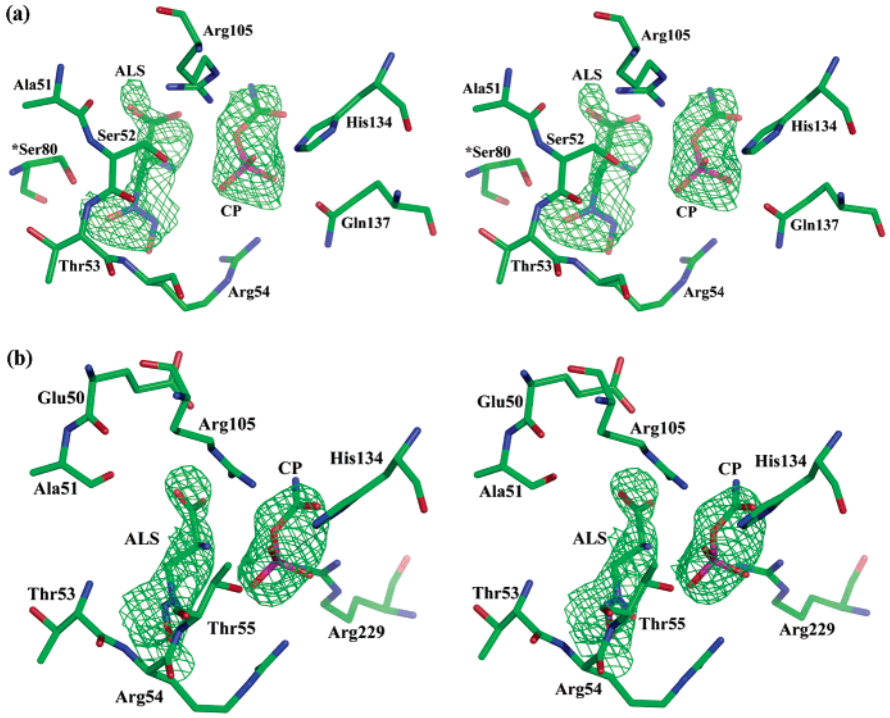

FIGURE 3: Stereo drawing of the active sites in aspartate transcarbamylase complexed with CP and L-alanosine: (a) chain A; (b) chain G. The $F_o - F_c$ omit electron density (2σ) around carbamyl phosphate (CP) and L-alanosine (ALS). Note that chains A and G are two catalytic chains in one asymmetric unit. The asterisk indicates the residue from the adjacent catalytic chain.

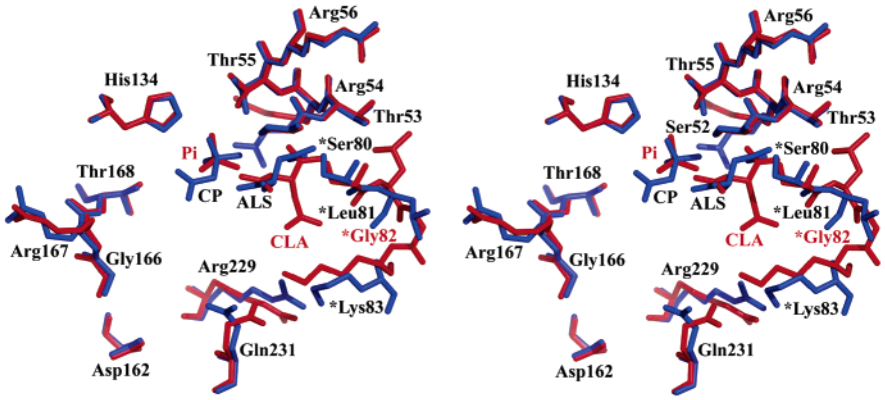

FIGURE 4: Stereo drawing of the superposition. The complex of CP and L-alanosine (ALS) with ATCase (blue) is superimposed onto the complex of carbamylaspartate (CLA) and phosphate with ATCase (red). The asterisk indicates the residue from the adjacent catalytic chain. Note that the phosphate of CP (blue) overlaps with the isolated phosphate (red) in the T-state position. The N_2O_2 of ALS (blue) overlaps with the α-CO_2^- of CLA (red), and the CO_2^- of ALS (blue) overlaps with the carbamyl group of CLA (red). The β-CO_2^- of CLA (red) does not overlap with ALS (blue).

DISCUSSION

T-State Binding Mode of Carbamyl Phosphate. The structures of ATCase ligated with *N*-phosphonacetyl-L-aspartate (PALA) (*19*) or carbamyl phosphate plus succinate (*14*) indicate the binding mode of carbamyl phosphate in the R-state. The binding of only carbamyl phosphate induces little conformation change of ATCase (*32*−*34*), which maintains the conformation of the enzyme in the T-state of the unligated enzyme. Thus ATCase undergoes a big conformational change only after the addition of the second substrate, L-aspartate. Is the binding mode of carbamyl phosphate in the T-state the same as that in the R-state? The answer is no. This new structure shows that the phosphate part of carbamyl phosphate has a similar binding mode with the phosphate (Figure 4) in ATCase complexed with carbamylaspartate plus phosphate (*35*). This phosphate site is about 4 Å away from that found in transition state analogues [PALA (*19*) or carbamyl phosphate plus succinate (*14*)]. The two phosphate sites 4 Å apart were previously identified in the complex of ATCase with pyrophosphate (*36*) or with phosphate at partial occupancy (*36*). The structure presented here indicates that carbamyl phosphate binds to the T-state ATCase in a different mode compared to the binding of carbamyl phosphate to the R-state. Therefore, a 4 Å movement of the phosphate of carbamyl phosphate occurs during the T to R transition as L-aspartate binds to ATCase. Further support for this binding mode of CP in the T-state of ATCase will need more T-state structures of ATCase bound to CP or its analogues along with aspartate or its analogues.

Different Binding Mode between L-Alanosine and L-Aspartate in ATCase Complexed with Carbamyl Phosphate. L-Alanosine acts as a pseudosubstrate for a number of L-aspartate-utilizing enzymes such as ATCase (*37*, *38*), L-aspartyl-tRNA synthetase (*39*), L-aspartate aminotransferase (*39*), and the L-aspartate transport system (*39*). In the interaction of L-alanosine with L-aspartate binding enzymes, it is usually suggested that L-alanosine and L-aspartate share a common binding site and thus possess common structural and chemical features. Surprisingly, this new structure shows that the binding mode of L-alanosine in the T-state (plus CP) is different from that of L-aspartate in the R-state (plus CP). Instead, L-alanosine occupies a position (Figure 4) which will be occupied by some part of product, carbamylaspartate. This unexpected binding mode of L-alanosine in the T form ATCase implies that L-alanosine acts somewhat like the product and its release will be easy like the product. In addition, aspartate (K_m = 11.8) (*40*) has higher affinity to ATCase than does L-alanosine (K_m > 1 M) (*10*). Thus, L-alanosine does not fully inhibit the binding of L-aspartate to native ATCase. This structural result is consistent with the early experimental result (*10*) that L-alanosine does not inhibit the carbamylation of L-aspartate in native ATCase at the same range of concentrations as in the case of the catalytic subunits. The fact (*10*) that L-alanosine did inhibit carbamylation of L-aspartate by the isolated catalytic subunit of *E. coli* ATCase can be reasonable if inhibition by L-alanosine is partly similar to product inhibition, which itself has been observed by Porter et al. (*32*) in kinetic studies of the ATCase catalytic subunit c_3. When the concentration for L-alanosine was varied from 2 to 100 mM, the optimum pH remained between 6.8 and 7.0 (*10*). Moreover, the saturation curve (*10*) of ATCase holoenzyme for L-alanosine shows a lack of homotropic cooperative interactions between the catalytic sites for the utilization of L-alanosine. Finally, similar T-state noncooperativity occurs in the reverse reaction study using products: carbamylaspartate and phosphate (*8*). Therefore, the binding mode of L-alanosine not only indicates that L-alanosine has a similar binding mode to that of some part of carbamylaspartate but also suggests that L-alanosine might behave at least partly like carbamylaspartate.

The result that the binding mode of L-alanosine in this new structure is somewhat different from that of L-aspartate suggests that L-alanosine might behave differently from L-aspartate as substrate for other L-aspartate-utilizing enzymes (*39*).

Orientation of Some Interesting Residues. Four residues, Arg54, Arg105, Arg167, and Arg229, which were previously identified as interacting with the bisubstrate analogue PALA (*19*, *41*, *42*), have been mutated by site-specific mutagenesis. Each of these mutants (*40*, *43*, *44*) showed approximately 900-fold or more reductions in the maximal observed specific activity and thus indicated that these four residues were critical for catalysis by ATCase.

Comparison of these four residues in the new structure and in other T- or R-state ATCase structures shows the following.

(a) The main chain of Arg54 moves slightly, and its backbone carbonyl oxygen is in contact with the hydroxyl group of *Tyr98 from the adjacent catalytic chain. This interaction between Arg54 (O) and *Tyr98 (OH) was also observed in the complex of the R-state, ATCase-PALA (*19*). The side chain of Arg54 interacts with Pro266, which is located in the 270s' loop (residues 265− 275). The interactions between some 270s'loop residues, Leu267 and Pro268, with Arg54 have been characterized in the unligated T-state ATCase (*30*). The interaction of Arg54 with the side chain of Gln137 is observed in the new structure.

(b) The side chain of Arg229 interacts with Pro268 (270s' loop) and *Lys83 (80s' loop, residues 76−85) from the adjacent catalytic chain. The interactions between Arg229 and the 270s' loop residues, Val270, Asp271, and Glu272, were observed in the complex of R-state ATCase-PALA or T-state ATCase-CLA-P_i (*35*). The interaction between Arg229 and *Lys84, another residue in the 80s' loop from the adjacent catalytic chain, was observed in the complex of R-state ATCase-PALA.

(c) The side chain of Arg167 interacts with Ser130 and His170. Both interactions were observed in the unligated T-state ATCase. In the new structure, the side chain of Arg167 interacts with Tyr197, which was also observed to contact with Arg167 in the T-state ATCase-AP-Asp; there is no interaction between Arg167 and either Glu50 or Arg234, both of which were observed in R-state ATCase-PALA.

(d) Residue Arg105 interacts with some 50s' loop (residues 47−53) residues (Cys47, Phe49, Glu50, Ala51, and Ser52) and Ala127. All of these interactions were observed in the unligated T-state ATCase or in the R-state ATCase-PALA. The two interactions (Arg105−His134 and Arg105−Arg167), which were observed in both the unligated T-state ATCase or R-state ATCase-PALA, were not present in the new structure.

It is clear that residues Arg54, Arg105, Arg167, and Arg229 must reorientate when substrates or their analogues bind to ATCase whether the enzyme is in the T-state or the R-state. Residues Arg105, Arg167, and Arg229 have been considered to model the substrate binding site in T-state ATCase (*45*). It has been indicated the Arg54 is essential for catalysis (*40*). When Arg54 was replaced by Ala (*40*), the holoenzyme and catalytic trimer subunit exhibited approximately 17000-fold and 70000-fold reductions in maximal activity, respectively.

Catalytic Mechanism for the Reaction of Carbamyl Phosphate with L*-Alanosine*. Although the binding modes of carbamyl phosphate and L-alanosine in this new structure are quite different from those of the corresponding parts in PALA (*19*) or carbamyl phosphate plus succinate (*14*) or phosphonoacetamide plus malonate (*46*), residues Arg105 and His134 still interact with the carbonyl oxygen of carbamyl phosphate. The distances between the phosphate oxygen (O_3P, Figure 5) of carbamyl phosphate and the amino nitrogen of L-alanosine are about 2.99 and 2.50 Å, respectively, in both active sites in one crystallographic asymmetric unit. In addition, the distances between the carbamyl carbon of carbamyl phosphate and the amino nitrogen of L-alanosine

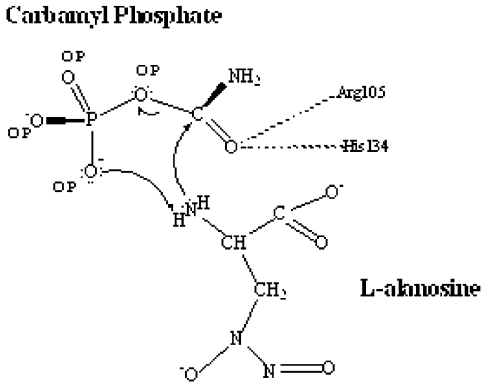

FIGURE 5: Probable mechanism for the reaction of carbamyl phosphate with L-alanosine catalyzed by ATCase.

are about 4.76 and 4.12 Å, respectively, in both active sites in one asymmetric unit. It is possible to suggest a mechanism (Figure 5), which is similar to the mechanism previous proposed for the reaction of CP and aspartate (*19*). The polarization of the carbonyl oxygen of carbamyl phosphate by His134 and Arg105 helps to form the tetrahedral intermediate (*41*, *47*). Then the removal of the proton from the NH_2 group of L-alanosine is accomplished by the leaving monophosphate dianion from carbamyl phosphate.

Summary. (1) The geometrical structure of ATCase bound to CP and L-alanosine is the T-state, not some intermediate state between T and R. The trimer $c_3\cdots c_3$ distance is 45.2 Å.

(2) The phosphate of CP in the ATCase-CP-ALS complex is 4 Å away from the position expected in the physiological ATCase-CP-Asp complex. This displacement was previously seen in ATCase bound to either pyrophosphate alone or phosphate alone.

(3) The L-alanosine binding mode is different from that of aspartate in the ATCase-CP-Asp complex and consistent with the kinetic result that alanosine did not inhibit the carbamylation of aspartate in the normal reaction of native ATCase plus carbamyl phosphate and aspartate. Instead, this normal reaction of native ATCase (c_6r_6 but not c_3) was moderately activated by alanosine (*10*).

(4) The anomaly (relative to aspartate) found in this X-ray diffraction study is the progressive binding of alanosine to the catalytic sites. This was suggested by both the mild stimulatory effect on the normal ATCase reaction (*3*) and the change in pH dependence of the alanosine reaction as its concentration is raised from 2 to 100 mM. This observation may be coupled with the high dissociation constant for alanosine (*10*) following the general coupling of reactions noted (*10*) by G. Weber (*48*, *49*). Further structural studies are thus indicated at various concentrations and pH values.

(5) The stimulation by PALA and the response to allosteric effectors of this T-state reaction are similar to those effects for other T-state reactions including the aspartate analogue, L-cysteinesulfinate (*9*), and the reverse reaction (*8*) of normal substrates under condition of rapid removal of one of the products: aspartate.

ACKNOWLEDGMENT

This work is based upon research conducted at the Cornell High Energy Synchrotron Source (CHESS), which is supported by the National Science Foundation under Award

DMR-0225180 and by the National Institutes of Health through its National Center for Research Resources under Award RR-01646.

REFERENCES

1. Wild, J. R., Johnson, J. L., and Loughrey, S. J. (1988) ATP-liganded form of aspartate transcarbamylase, the logical regulatory target for allosteric control in divergent bacterial systems, *J. Bacteriol. 170*, 446−448.
2. Gerhart, J. C., and Pardee, A. B. (1964) Aspartate transcarbamylase, an enzyme designed for feedback inhibition, *Fed. Proc. 23*, 727−735.
3. Thiry, L., and Hervé, G. (1978) The stimulation of *Escherichia coli* aspartate transcarbamylase activity by adenosine triphosphate, *J. Mol. Biol. 125*, 515−534.
4. Tauc, P., Leconte, C., Kerbiriou, D., Thiry, L., and Hervé, G. (1982) Coupling of homotropic and heterotropic interactions in *Escherichia coli* aspartate transcarbamylase, *J. Mol. Biol. 155*, 155−168.
5. Leger, D., and Hervé, G. (1988) Allostery and pK_a changes in aspartate transcarbamylase from *Escherichia coli*: analysis of the pH dependence in the isolated catalytic subunits, *Biochemistry 27*, 4293−4298.
6. Pastra-Landis, S. C., Evans, D. R., and Lipscomb, W. N. (1978) The effect of pH on the cooperative behavior of aspartate transcarbamylase from *Escherichia coli*, *J. Biol. Chem. 253*, 4624−4630.
7. Hervé, G., Schmitt, B., and Serre, V. (2004) Cooperativity and high pressure: stabilization of the R conformation of the allosteric aspartate transcarbamylase under the influence of pressure, *Cell. Mol. Biol. 50*, 347−352.
8. Foote, J., and Lipscomb, W. N. (1981) Kinetics of aspartate transcarbamylase from *Escherichia coli* for the reverse direction of reaction, *J. Biol. Chem. 256*, 11428−11433.
9. Foote, J., Lauritzen, A. M., and Lipscomb, W. N. (1985) Substrate specificity of aspartate transcarbamylase: interaction of the enzyme with analogs of aspartate and succinate, *J. Biol. Chem. 260*, 9624−9629.
10. Baillon, J., Tauc, P., and Hervé, G. (1985) L-alanosine: a non-cooperative substrate for *Escherichia coli* aspartate transcarbamylase, *Biochemistry 24*, 7182−7187.
11. Murthy, Y. K. S., Thiemann, J. E., Coronelli, C., and Sensi, P. (1966) Alanosine, a new antiviral and antitumor agent isolated from a *Streptomyces*, *Nature 211*, 1198−1199.
12. Nowlan, S. F., and Kantrowitz, E. R. (1985) Superproduction and rapid purification of *E. coli* aspartate transcarbamoylase and its catalytic subunit under extreme derepression of the pyrimidine pathway, *J. Biol. Chem. 260*, 14712−14716.
13. Xu, W., Pitts, M. A., Middleton, S. A., Kelleher, K. S., and Kantrowitz, E. R. (1988) Propagation of allosteric changes through the catalytic-regulatory interface of *Escherichia coli* aspartate transcarbamylase, *Biochemistry 27*, 5507−5515.
14. Gouaux, J. E., and Lipscomb, W. N. (1988) Three-dimensional structure of carbamoyl phosphate and succinate bound to aspartate carbamoyltransferase, *Proc. Natl. Acad. Sci. U.S.A. 85*, 4205−4208.
15. Jones, M. E. (1963) Carbamyl phosphate: many forms of life use this molecule to synthesize arginine, uracil, and adenosine triphosphate, *Science 140*, 1373−1379.
16. Allen, C. M., and Jones, M. E. (1964) Decomposition of carbamyl phosphate in aqueous solutions, *Biochemistry 3*, 1238−1247.
17. Halmann, M., Lapidot, A., and Samuel, D. (1962) Kinetic and tracer studies of the reactions of carbamoyl phosphate in aqueous solution, *J. Chem. Soc. 84*, 1944−1957.
18. Shi, D., Morizono, H., Yu, X., Tong, L., Allewell, N. M., and Tuchman, M. (2001) Human ornithine transcarbamylase: crystallographic insights into substrate recognition and conformational changes, *Biochem. J. 354*, 501−509.
19. Jin, L., Stec, B., Lipscomb, W. N., and Kantrowitz, E. R. (1999) Insights into the mechanisms of catalysis and heterotropic regulation of *Escherichia coli* aspartate transcarbamoylase based upon a structure of the enzyme complexed with the bisubstrate analogue *N*-phosphonacetyl-L-aspartate at 2.1 Å, *Proteins: Struct., Funct., Genet. 37*, 729−742.
20. Navaza, J. (1994) AMoRe: an automated package for molecular replacement, *Acta Crystallogr. A50*, 157−163.
21. Shi, D., Morizono, H., Aoyagi, M., Tuchman, M., and Allewell, N. M. (2000) Crystal structure of human ornithine transcarbamylase complexed with carbamoyl phosphate and L-norvaline at 1.9 Å resolution, *Proteins: Struct., Funct., Genet. 39*, 271−277.
22. Jalal, M. A. F., Hossain, M. B., and Helm, D. V. D. (1986) Structure of anticancer antibiotic L-alanosine, *Acta Crystallogr. C42*, 733−738.
23. Brunger, A. T., Adams, P. D., Clore, G. M., DeLano, W. L., Gros, P., Grosse-Kunstleve, R. W., Jiang, J. S., Kuszewski, J., Nilges, N., Pannu, N. S., Read, R. J., Rice, L. M., Simonson, T., and Warren, G. L. (1998) Crystallography and NMR system (CNS): A new software system for macromolecular structure determination, *Acta Crystallogr. D54*, 905−921.
24. Jones, T. A, Zou, J. Y., Cowan, S. W., and Kjeldgaard, M. (1991) Improved methods for building protein models in electron density maps and the location of errors in these models, *Acta Crystallogr. A47*, 110−119.
25. Laskowski, R. A., MacArthur, M. W., Moss, D. S., and Thornton, J. M. (1993) PROCHECK: A program to check the stereochemical quality of protein structures, *J. Appl. Crystallogr. 26*, 283−291.
26. Jones, S., and Thornton, J. M. (1996) Principles of protein−protein interactions derived from structural studies, *Proc. Natl. Acad. Sci. U.S.A. 93*, 13−20.
27. Delano, W. N. (2002) The PyMOL molecular graphic system, Delano Scientific, San Carlos, CA.
28. Williams, M. K., Stec, B., and Kantrowitz, E. R. (1998) A single mutation in the regulatory chain of *Escherichia coli* aspartate transcarbamoylase results in an extreme T-state structure, *J. Mol. Biol. 281*, 121−134.
29. Kleywegt, G. J. (1999) Experimental assessment of differences between related protein crystal structures, *Acta Crystallogr. D55*, 1878−1884.
30. Stevens, R. C., Gouaux, J. E., and Lipscomb, W. N. (1990) Structural consequences of effector binding to the T state of aspartate carbamoyltransferase: crystal structures of the unligated and ATP- and CTP-complexed enzymes at 2.6 Å resolution, *Biochemistry 29*, 7691−7701.
31. Kantrowitz, E. R., and Lipscomb, W. N. (1990) *Escherichia coli* aspartate transcarbamoylase: the molecular basis for a concerted allosteric transition, *Trends Biochem. Sci. 15*, 53−59.
32. Porter, R. W., Modebe, M. O., and Stark, G. R. (1969) Aspartate transcarbamylase: kinetic studies of the catalytic subunit, *J. Biol. Chem. 244*, 1846−1859.
33. Wedler, F. C., and Gasser, F. J. (1974) Ordered substrate binding and evidence for a thermally induced change in mechanism for *E. coli* aspartate transcarbamylase, *Arch. Biochem. Biophys. 163*, 57−68.
34. Jacobson, G. R., and Stark G. R. (1975) Aspartate transcarbamylase of *Escherichia coli*: mechanisms of inhibition and activation by dicarboxylic acids and other anions, *J. Biol. Chem. 250*, 6852−6860.
35. Huang, J., and Lipscomb, W. N. (2004) Products in the T-state of aspartate transcarbamylase: crystal structure of the phosphate and *N*-carbamyl-L-aspartate ligated enzyme, *Biochemistry 43*, 6422−6426.
36. Honzatko, R. B., and Lipscomb, W. N. (1982) Interactions of phosphate ligands with *Escherichia coli* aspartate carbamoyltransferase in the crystalline state, *J. Mol. Biol. 160*, 265−286.
37. Gale, G. R., Ostrander, W. E., and Atkins, L. M. (1968) Effects of alanosine on purine and pyrimidine synthesis, *Biochem. Pharmacol. 17*, 1823−1832.
38. Jayaram, H. N., and Cooney, D. A. (1979) Analogs of L-aspartic acid in chemotherapy for cancer, *Cancer Treat. Rep. 63*, 1095−1108.
39. Anandaraj, S. J., Jayaram, H. N., Cooney, D. A., Tyagi, A. K., Han, N., Thomas, J. H., Chitnis, M., and Montgomery, J. A. (1980) Interaction of L-alanosine (NSC 153,353) with enzymes metabolizing L-aspartic acid, L-glutamic acid, and their amides, *Biochem. Pharmacol. 29*, 227−245.
40. Stebbins, J. W., Xu, W., and Kantrowitz, E. R. (1989) Three residues involved in binding and catalysis in the carbamyl phosphate binding site of *Escherichia coli* aspartate transcarbamylase, *Biochemistry 28*, 2592−2600.
41. Huang, J., and Lipscomb, W. N. (2004) Aspartate transcarbamylase (ATCase) of *Escherichia coli*: a new crystalline R-state bound to PALA, or to product analogues citrate and phosphate, *Biochemistry 43*, 6415−6421.

42. Krause, K. L., Voltz, K. W., and Lipscomb, W. N. (1987) 2.5 Å structure of aspartate carbamoyltransferase complexed with the bisubstrate analog *N*-(phosphonacetyl)-L-aspartate, *J. Mol. Biol. 193*, 527−553.
43. Stebbins, J. W., Zhang, Y., and Kantrowitz, E. R. (1990) Importance of residues Arg-167 and Gln-231 in both the allosteric and catalytic mechanisms of *Escherichia coli* aspartate transcarbmoylase, *Biochemitry 29*, 3821−3827.
44. Middleton, S. A., Stebbins, J. W., and Kantrowitz, E. R. (1989) A loop involving catalytic chain residues 230−245 is essential for the stabilization of both allosteric forms of *Escherichia coli* aspartate transcarbamylase, *Biochemistry 28*, 1617−1626.
45. Cherfils, J., Vachette, P., and Janin, J. (1990) Modelling allosteric processes in *E. coli* aspartate transcarbamylase, *Biochimie 72*, 617−624.
46. Gouaux, J. E., Stevens, R. C., and Lipscomb, W. N. (1990) Crystal structures of aspartate carbamoyltransferase ligated with phosphonoacetamide, malonate, and CTP or ATP at 2.8 Å resolution and neutral pH, *Biochemistry 29*, 7702−7715.
47. Lipscomb, W. N. (1994) Aspartate transcarbamylase from *Escherichia coli:* Activity and regulation, *Adv. Enzymol. Relat. Areas Mol. Biol. 68*, 67−151.
48. Weber, G. (1984) Order of free energy couplings between ligand binding and protein subunit association in hemoglobin, *Proc. Natl. Acad. Sci. U.S.A. 81*, 7098−7102.
49. Weber, G. (1975) Energetics of ligand binding to proteins, *Adv. Protein Chem. 29*, 1−83.

BI051543U